Tetrahedron 69 (2013) 8051–8063

Contents lists available at SciVerse ScienceDirect

Tetrahedron

journal homepage: www.elsevier.com/locate/tet

Experimental and computational study of the complexation of adamantyl glycosides with β-cyclodextrin

Željka Car †, Ivan Kodrin †, Josip Požar †, Rosana Ribić, Davor Kovačević, Vesna Petrović Peroković *

Department of Chemistry, Faculty of Science, University of Zagreb, Horvatovac 102a, HR-10000 Zagreb, Croatia

ARTICLE INFO

Article history:
Received 30 November 2012
Received in revised form 12 June 2013
Accepted 27 June 2013
Available online 4 July 2013

Keywords:
Adamantyl glycoconjugates
β-Cyclodextrin
Inclusion complexes
Microcalorimetry
Molecular modelling
NMR studies

ABSTRACT

Complexation of α- and β-anomers of adamantyl galactosides and adamantyl mannosides, having different configuration of the chiral linker connecting the sugar and the adamantamine (AMA) subunits, with β-cyclodextrin (β-CD) was investigated by means of NMR spectroscopy, microcalorimetric titrations and computational studies. The synthesis of adamantyl galactosides is also reported.

The experimental investigations are consistent with the formation of 1:1 complexes in which the hydrophilic part of the guest protruded out of the secondary rim. The β-cyclodextrin was shown to be a rather efficient binder for the examined guests in water, primarily as a consequence of the enthalpically favourable inclusion of the adamantyl moiety within the hydrophobic cavity of the host.

The structures of AMA derivatives complexes were modelled by combination of molecular and quantum mechanics - B3LYP/6-31G(d) in implicitly modelled water (PCM). The differences in the stability of primary and secondary complexes were observed. The main reasons for that could be more pronounced dehydration of the hydrophilic part of the guest upon complete adamantane inclusion in the complexes of primary type and the different hydrogen bonding pattern at the primary and secondary CD rims.

1. Introduction

Cyclodextrins (CDs) are cyclic oligosaccharides comprised of (α-1,4)-linked α-D-glucopyranose units with a truncated cone shape and characteristic lipophilic central cavity. Naturally occurring CDs are of α, β and γ types, containing six, seven and eight glucopyranose units, respectively.[1] During the past few decades, these macrocyclic receptors have been extensively studied because of their ability to host wide variety of hydrophobic compounds and hydrophobic moieties of amphiphilic molecules in water.[2,3] The embedding of lipophilic groups within cyclodextrins is primarily attributed to hydrophobic hydration of both host and guest cavities and, to a lesser extent, the van der Waals interactions realized upon inclusion.[3,4] In addition, the hydrophilic part of an amphiphilic guest can often be involved in hydrogen bonding with the hydroxyl groups of host, located at both secondary (wide) and primary (narrow) rim of macrocyclic ring.[3,4] This can in turn influence the penetration depth of hydrophobic groups within the macrocycle and the structure of complex (the protrusion of hydrophilic moiety out of the secondary or the primary rim).[3,4]

Among the variety of hydrophobic groups, which can be embedded into the most frequently investigated β-CD (Fig. 1), the inclusion of adamantyl residue, with its nearly spherical shape and the radius almost perfectly fitting in the host cavity,[5] is quite favourable. Indeed, the efficient binding of several adamantane derivatives by β-CD has been documented in the literature.[5–15] Most of the work done was primarily focused on the complexation thermodynamics,[5,11–14] while the structure of the complexes formed (i.e., the position of the hydrophilic part of guest with respect to the primary and to the secondary rim of macrocycle) was less frequently explored.[6,7,10]

The understanding of all the factors leading to thermodynamically advantageous binding of adamantane-based compounds with β-CD is held to be of great importance. These complexes are often considered as model compounds, the stability of which can, at least partially, explain the affinity of adamantane towards cell membranes and hydrophobic compounds in general. This is becoming ever more significant because adamantane-based molecules have a potential use as therapeutics for viral infections, neurodegenerative disorders, type 2 diabetes, cancer and other diseases, presumably due to their lipophilic properties.[16] Moreover, the covalent attachment of the adamantyl group to several drug molecules seems to notably enhance their bioavailability.[16]

Additionally to the experimental investigations, considerable efforts directed towards the computational modelling of cyclodextrins and their inclusion complexes have been made. Typically,

* Corresponding author. Tel.: +385 1 4646409; fax: +385 1 4606401; e-mail address: vpetrovi@chem.pmf.hr (V.P. Peroković).
† These authors contributed equally to the work.

0040-4020/$ – see front matter © 2013 Elsevier Ltd. All rights reserved.
http://dx.doi.org/10.1016/j.tet.2013.06.097

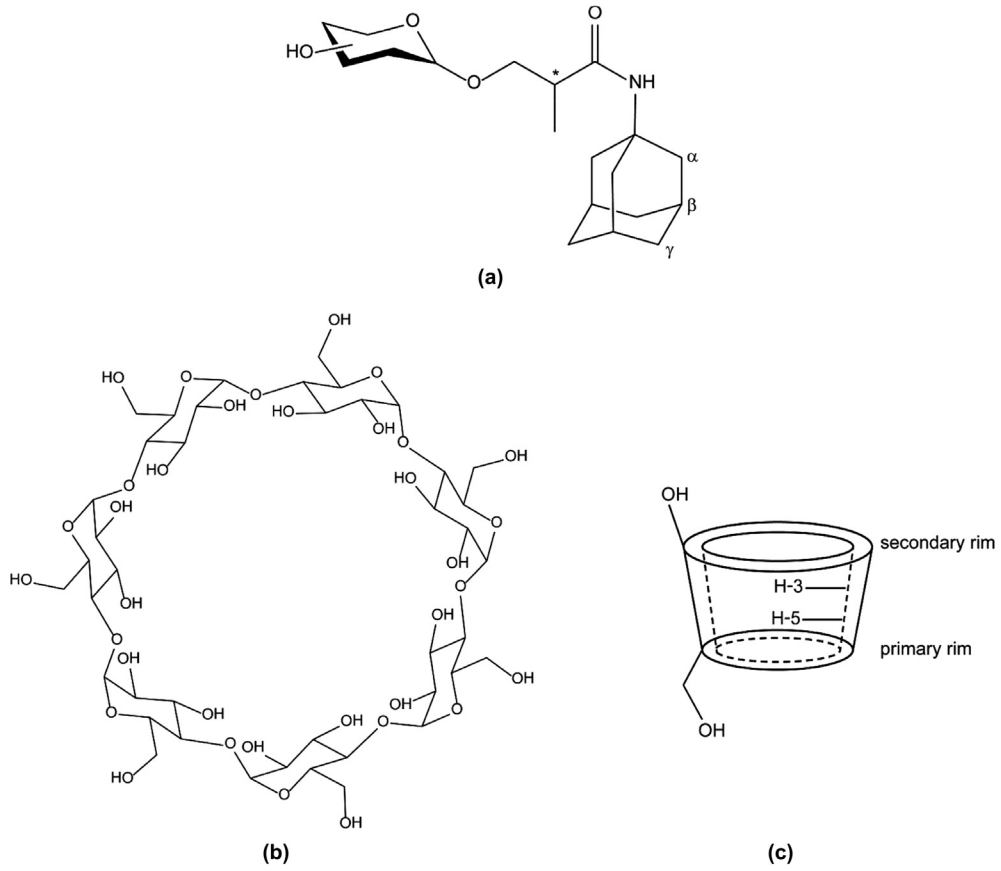

Fig. 1. (a) General structure of the guest molecules. (b) Structural formula of the host, β-CD. (c) Truncated cone shape model of β-CD.

structure, energy and thermodynamic functions of host, guest and corresponding complexes are reported, most often in vacuo.[17–19] Such large molecules are quite often treated with molecular mechanics and semi-empirical methods.[20] However, the computationally more expensive density functional theory (DFT) is becoming more frequently used, especially when the interactions between guest and cyclodextrins are of interest.[21] Recently, computational investigations of the complexes of several pharmaceutical compounds with β-CD have been performed in the solvent modelled as polarizable continuum.[22]

Our interest is especially focused on the glycoconjugates containing monosaccharides such as mannose, galactose, *N*-acetylgalactosamine and *N*-acetylglucosamine, which can serve as recognition determinants in specific recognition of glycoconjugates by lectins.[23] In the framework of our research, we have previously reported the synthesis of several adamantane-derived *O*-mannosides.[24,25] These biologically active compounds should be especially suited for complexation with β-CD in water due to the fact that in addition to the expected adamantane inclusion within the hydrophobic cavity, the hydrophilic part of guest can be involved in the favourable hydrogen bonding with the macrocycle.[8,9] We have therefore synthesized adamantyl galactosides and decided to study the binding of adamantyl glycoconjugates, namely α- and β-anomers of adamantyl galactosides and adamantyl mannosides with different configuration of chiral linker connecting the sugar and the adamantamine (AMA) subunits (Fig. 1), with β-cyclodextrin by an integrated experimental and computational approach.

The computational study was performed to address the possible conformers of 1:1 inclusion complexes and to explore the complexation energetics. The main goal of the experimental research was to explore the structure of the complexes and to investigate the corresponding reaction thermodynamics. For that purpose, NMR (^{1}H and ROESY) and microcalorimetric investigations were performed. Finally, the theoretical results were compared with the experimental findings.

2. Results and discussion

2.1. Synthesis of AMA galactoconjugates

AMA galactoconjugates (Scheme 1) were prepared according to the procedure previously described for analogous *O*-mannosyl derivatives.[24] Benzylated α,β-D-galactopyranosyltrichloroacetimidate was used as glycosyl donor.[26] O-Galactosylation of methyl (*R*)- or (*S*)-3-hydroxy-2-methylpropionate was promoted by the catalytic amount of boron trifluoride diethyl etherate ($BF_3 \cdot Et_2O$) in dichloromethane at 0 °C. Under specified reaction conditions trichloroacetimidate-mediated *O*-glycosylations gave anomeric mixtures of the corresponding *O*-galactosides **1**α,β (61%) and **2**α,β (65%). In both mixtures the α/β ratio was 2:1. Pure anomers **1**α, **1**β, **2**α and **2**β were obtained by column chromatography on silica gel.

The hydrolysis of methyl esters of each anomer **1** and **2** was performed by saponification leading to 79–84% yield of acids **3** and **4**. The next step was the activation of the free carboxyl group and condensation with AMA using EDC·HCl/HOBt coupling reagents for amide bond formation. Glycoconjugates **5** and **6** were obtained in good yield (55–66%). Debenzylation of compounds **5** and **6** was performed by catalytic hydrogenolysis and gave the desired AMA conjugates **7** and **8** (91–95%).

The complexation of galactosyl conjugates (**7**α, **7**β, **8**α and **8**β) and the analogous mannose derivatives (**9**α, **9**β, **10**α and **10**β,

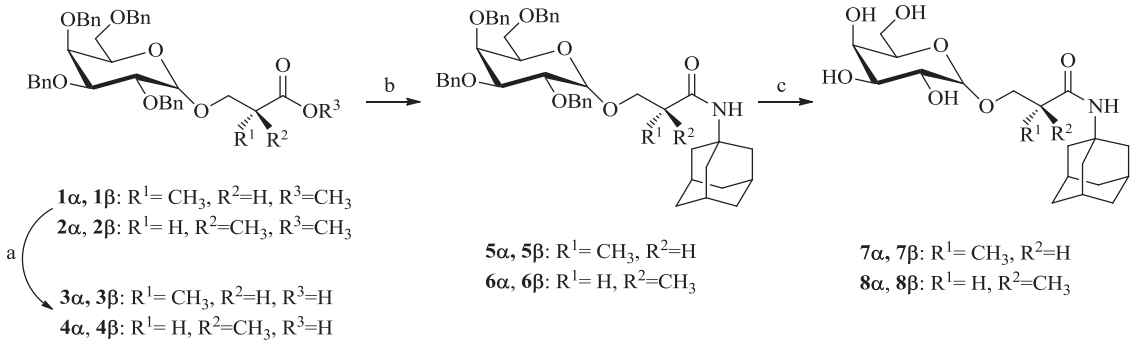

Scheme 1. Synthesis of galactose–AMA derivatives: (a) NaOH (1 M), dioxane, 79–84% yield; (b) (i) EDC·HCl, Et_3N, dry CH_2Cl_2; (ii) HOBt·H_2O; (iii) AMA·HCl, Et_3N, 55–66% yield; (c) H_2 (4 bar), Pd/C (10%), CH_3OH, 91–95% yield.

Fig. 2)[24] with β-CD was investigated by means of NMR, microcalorimetric titrations and DFT based computational studies.

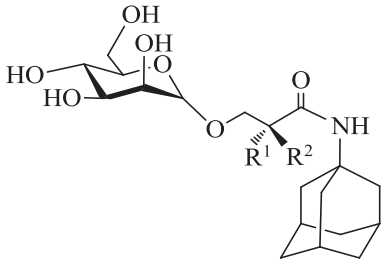

9α, 9β: R^1= CH_3, R^2=H
10α, 10β: R^1= H, R^2=CH_3

Fig. 2. Structures of mannose–AMA derivatives.

2.2. NMR investigations

The structure of the supramolecular complexes formed from the prepared guest molecules and β-CD in water was investigated by means of NMR. As an example of the results obtained, the ^{1}H NMR spectra of the **8**β glycoconjugate upon cyclodextrin addition are given in Fig. 3. By inspecting the presented data it can be seen that upon going from the pure guest to the 2:1 molar ratio of added β-CD with respect to glycoconjugate, the signals of all protons on the adamantane subunit (Hα, Hβ and Hγ) of **8**β experience a downfield shift. The addition of the host is accompanied by changes in the shape of the methylene Hγ signal on the AMA subunit from a broad singlet to what appears to be two separate doublets. On the other hand, no significant changes in the position and the signal shape of the other guest protons upon host addition could be observed. Only the relatively small, downfield chemical shift displacement of the linker protons of the glycoconjugates was noticed. The complexation of guest molecule with the host was also evident from the changes in the resonance spectra of cyclodextrin. An appreciable upfield shift of resonant signals of the protons situated within the cavity (H-3 and H-5) in the presence of the **8**β occurred. The described results indicate that the complexation is primarily realized by the inclusion of the hydrophobic part of guest molecules within the cavity of the macrocycle. This is in accord with the results reported for complexes of adamantyl derivatives with β-CD in water, the structure of which was investigated by means of NMR.[6,7]

The stability constant of the 1:1 complex formed (**8**β·CD), was calculated by processing the collected NMR titration data using HypNMR2006 software. The obtained value (log K=4.1) indicates

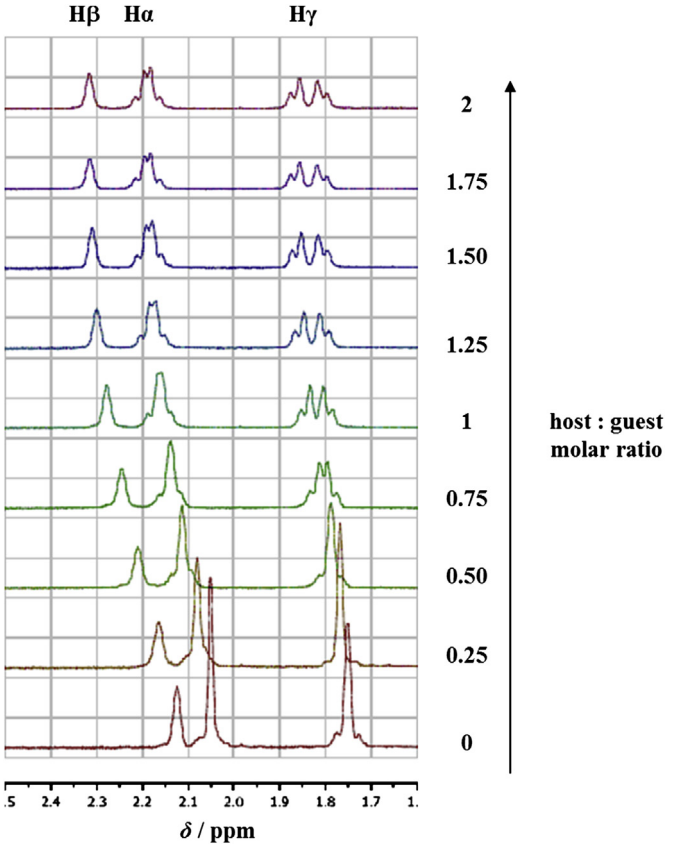

Fig. 3. ^{1}H NMR spectra of adamantane region of **8**β upon β-CD addition in D_2O at ϑ=25.0 °C.

thermodynamically advantageous inclusion of the hydrophobic subunit into the host cavity. The formation of stable 1:1 complexes (4.5≤log K≤4.6) with all investigated guests was confirmed by means of titration calorimetry (Section 2.3), which was used for detailed thermodynamic investigations of the complexation reactions. The reason for the choice of this technique lies in the fact that this experimental technique, unlike NMR, it allows for the simultaneous determination of all standard thermodynamic functions of complexation ($\Delta_cG°$, $\Delta_cH°$, $\Delta_cS°$) from only one titration experiment.

To deduce the structure of the complexes formed with all other examined guest molecules the ^{1}H NMR spectra of the reaction mixture at 2:1 host to guest ratio and similar concentrations of both reactants as in the previously described experiment were recorded. The obtained results with the galactosyl conjugates (**7**α, **7**β, **8**α and

8β) and the analogous mannosyl derivatives (**9**α, **9**β, **10**α and **10**β) at the above molar ratio of reactants can be summarized as follows. The addition of the host to the examined guests led to qualitatively and quantitatively almost identical changes in the spectra of both reactants as in the case of **8**β, irrespectively of the sugar type and the absolute configuration of the chiral linker atom. This is clearly illustrated by the changes in the chemical shifts of the adamantane protons observed upon macrocycle addition (Δδ), which are enlisted in Table 1. Consequently, we suggest that the structure of all the reaction products is quite similar to the structure of the **8**β·CD complex.

Table 1
The difference in the chemical shifts (Δδ) of the guest AMA protons between the complex (at 2:1 host to guest molar ratio) and the pure guest at ϑ=25.0 °C in D_2O (c(guest)=3×10^{-3} mol dm^{-3})

Guest	Δδ (AMA)		
	Hγ (CH_2)	Hα (CH_2)	Hβ (CH)
7α	0.10	0.13	0.20
7β	0.09	0.14	0.20
8α	0.08	0.15	0.19
8β	0.09	0.14	0.19
9α	0.09	0.14	0.19
9β	0.08	0.15	0.19
10α	0.09	0.14	0.19
10β	0.09	0.14	0.19

In principle, much lower changes in the resonant frequencies of the linker and the sugar protons of the guest do not a priori exclude the hydrogen bonding of suitable donor and acceptor atoms in the hydrophilic part of AMA glycoconjugates and the hydroxyls of the macrocycle. To shed more light on the structure of the complexes formed, particularly to deduce the position of the sugar moiety and the linker atoms with respect to the macrocycle, the Rotating-frame Overhauser Effect Spectroscopy (ROESY) was employed. In the recent study,[7] the ROESY technique was successfully applied for resolving the structure of the complexes of covalently modified cyclodextrins and rimantidine. A notable difference in spectra of solution prepared by mixing the reactants was noticed, depending on whether the hydrophilic part of guest protruded out of the primary or out of the secondary rim of macrocycle (i.e., whether the primary or the secondary complex was formed). The formation of the secondary complex resulted in visible cross peaks between all adamantane protons and H-3 and H-5 protons of macrocycle, indicating the deep inclusion of this group within the cavity of the host. By contrast, the inclusion of the adamantane with the hydrophilic moiety situated at the primary rim (complex of the primary type) was more partial. Only the cross peaks between Hβ and Hγ and the H-3 and H-5 protons of CD were visible. Additionally, the cross peaks between the methyl protons of the guest and H-3 and H-5 protons of macrocycle were of weak intensity in the case of both the primary and the secondary complexes, suggesting only partial dehydration of hydrophilic part of the guest.[7] Expectedly, the secondary complex was more stable than the primary one.

Since the results of ^{1}H NMR investigations indicated that all the herein reported adducts of β-CD and AMA glycoconjugates have similar structures, the ROESY experiments were performed only in the case of **10**α and **10**β derivatives. As an example of obtained results, the spectrum recorded upon the addition of host to **10**β (1:1 molar ratio) is shown in Fig. 4.

The clearly visible cross peaks between H-3 and H-5 protons of the host and all the protons of AMA subunit (Hα, Hβ and Hγ, Fig. 1) confirm the deep inclusion of adamantane into the hydrophobic cavity of the β-CD. On the other hand, the absence of strong cross peaks between the signals of the linker protons of both derivatives and those of the cyclodextrin indicates larger distances between the atoms in the hydrophilic part of guest and the atoms of the macrocycle. Consequently, the hydrophilic part of the guest molecule and the hydroxyl groups of β-CD most likely remain partially hydrated upon complexation. Their participation in the complexation process can therefore be characterized as weak.

By taking into account the results of the herein reported NMR investigations, as well as the results of Tato et al.,[7] one could conclude that the complexes between the examined guests and cyclodextrin are of secondary type. Namely, the inclusion of adamantane subunit of the examined glycoconjugates into the cavity of the macrocycle was found to be almost complete, as in the case of the secondary rimantidine adducts with β-CD. Likewise, no significant involvement of the hydrophilic part of the examined glycoconjugates and the macrocycle in the hosting process could be observed.

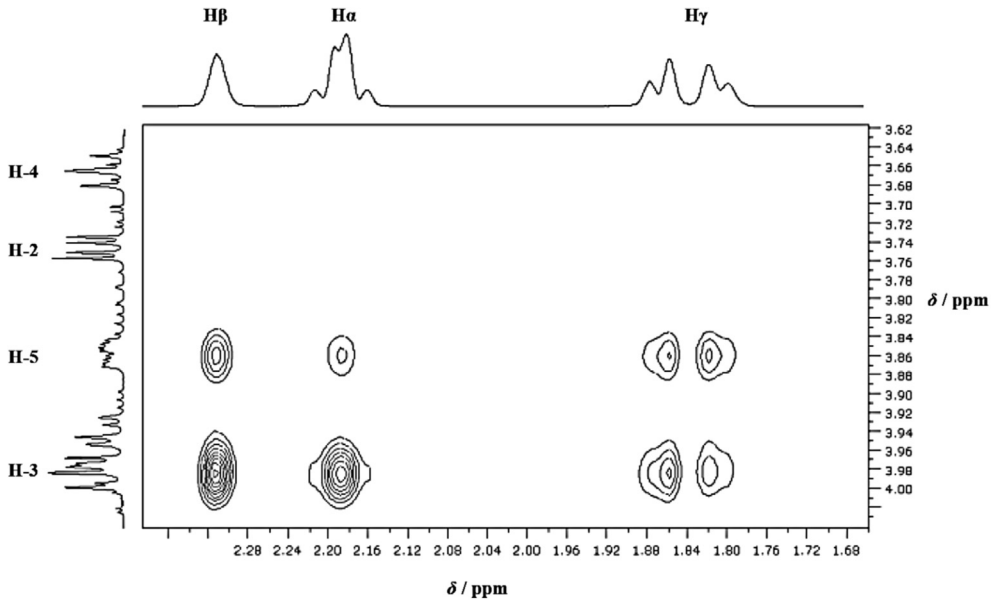

Fig. 4. Partial contour plot of the ROESY spectrum of the reaction mixture containing **10**β and β-CD (molar ratio 1:1) at ϑ=25.0 °C in D_2O.

2.3. Microcalorimetry

The microcalorimetric titrations of examined guests with the host were performed in order to investigate the thermodynamics of the corresponding reactions. As an example of obtained results, a thermogram recorded by titrating **10**β with cyclodextrin at 25 °C is shown in Fig. 5a. The stepwise addition of β-CD resulted in exothermic enthalpy changes, which was also the case for all other adamantyl glycoconjugates reported in this paper. The formation of 1:1 complexes was observed for all investigated glycoconjugates. The standard reaction enthalpy and the equilibrium constant (hence the standard reaction Gibbs energy) for the complexation of guest molecule with the macrocycle were calculated by a least-squares non-linear regression analysis of calorimetric titration data (Fig. 5b). Standard complexation entropy was calculated from the complexation enthalpy and Gibbs energy.

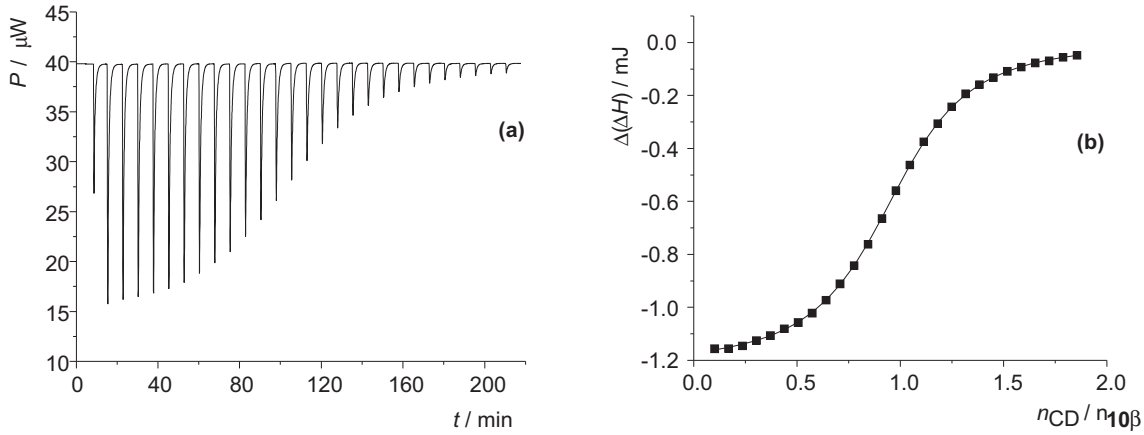

Fig. 5. (a) Thermogram of the microcalorimetric titration of **10**β (c_0=6×10^{-4} mol dm^{-3}, V_0=1.42 mL) with CD (c=5×10^{-3} mol dm^{-3}) in water; ϑ=(25.0±0.1) °C. (b) The dependence of successive enthalpy changes on host to guest molar ratio. ■ experimental; – calculated.

The obtained thermodynamic parameters are given in Table 2. The presented data indicate that the complexation process is favourable both in terms of standard reaction enthalpy and entropy, leading to relatively high affinity of the macrocycle towards investigated guests. However, the enthalpic contribution to the Δ_cG° is notably larger than the entropic one. Evidently, no considerable influence of the sugar part of glycoconjugates and the configuration of chiral linker atom on the thermodynamic parameters of complexation could be observed. The values of the standard reaction parameters are quite similar, irrespective of the type of the hydrophilic group covalently attached to adamantyl unit.

Table 2
Thermodynamic parameters of complexation of adamantyl glycoconjugates with β-CD in water; ϑ=(25.0±0.1) °C

Guest	log K±SE	(Δ_rH°/kJ mol^{-1})±SE	(Δ_rS°/J K^{-1} mol^{-1})±SE
7α	4.549±0.004	−23.42±0.09	8.5±0.4
7β	4.617±0.004	−19.73±0,05	22.5±0.4
8α	4.497±0.004	−21.88±0.06	12.7±0.1
8β	4.552±0.002	−22.88±0.02	10.38±0.08
9α	4.511±0.003	−18.83±0.06	23.2±0.1
9β	4.603±0.003	−22.34±0.07	13.2±0.2
10α	4.474±0.008	−18.24±0.07	24.5±0.3
10β	4.577±0.005	−21.9±0.1	14.1±0.5

SE=standard error of the mean (N=3–4).

As noted in the previous chapter, the NMR experiments revealed that the adamantane inclusion results with the formation of the secondary complex in which the hydrophilic part of the guest, most likely, forms hydrogen bonds with water molecules. The weaker participation of the linker atoms and the sugar subunits in the hosting process is evident from the standard reaction parameters, which are very close to the corresponding values for the secondary rimantidine complex, also characterized by the weak involvement of the guest amino group in the complexation process.[7]

In general, the thermodynamically advantageous inclusion of adamantane within the hydrophobic cavity of β-CD is, by large, held to be the result of displacement of the 'high energy' water molecules (with respect to water molecules in liquid) situated within the hydrophobic cavity of host and the favourable adamantane dehydration.[3,4,27] Because of the saturated hydrocarbon structure of the host cavity and adamantane, only the relatively weak dispersive interactions between host and guest can be expected, which are most likely not favourable enough to account for the reported reaction enthalpies. Though it should be noted that because of the large size of the guest and the cavity, their portion in Δ_rH° is certainly not negligible.[5]

Recent MD investigations of cyclodextrin structure and hydration energetics support the thesis regarding high energy water molecules within the cavity.[28] The extent of hydrogen bonding within the macrocycle was noticed to be considerably lower than in the bulk. The endothermic transfer enthalpies ($\Delta_{tr}H^\circ$) of adamantane from the unstructured to the hydrogen bonding solvents ($\Delta_{tr}H^\circ$ of adamantane from cyclohexane to ethanol and methanol are 4.08 kJ mol^{-1} and 6.80 kJ mol^{-1}, respectively)[29] indicate that its dehydration could be exothermic since the enthalpies of adamantane transfer among unstructured solvents (*n*-hexane, cyclohexane, carbon tetrachloride) are all very close to zero.[30] This might, combined with the displacement of 'high energy' water molecules explain the favourable complexation enthalpies.

On the other hand, the classical view on the hydrophobic solvation suggests the enthalpically favourable formation of the *clathrate*-like water cages around lipophilic solute molecules.[31,32] If that is the case the dehydration of the organic compounds like adamantane should be entropically favoured and enthalpically disfavoured.[27,31,32] Consequently, the enthalpically advantageous inclusion of adamantane in that case can be ascribed to the displacement of the high energy water molecules from the cavity and the realized dispersive interactions. Likewise, the low standard reaction enthalpy could be due to the favourable adamantane dehydration, and the entropically unfavourable release of the water molecules situated within the cavity of the macrocycle.

To conclude, the results of the carried out experimental investigations indicate that the release of water molecules situated within the cavity of β-CD and the thermodynamically favourable dehydration of adamantane subunit as well as the dispersive

interactions realized can be considered as the most important factors, which determine the stability of investigated inclusion complexes.

2.4. Computational studies

The main goal of the performed computational studies was to obtain an insight in the possible structures of the complexes between the examined guest molecules and β-CD. Namely, the majority of the literature data suggest the formation of complexes with deeply embedded adamantyl moiety, usually protruding out of the wider secondary rim of CD. This experimental finding is usually explained by the truncated cone shape of the macrocycle, which prevents the deep inclusion of adamantane in primary complexes. However, quite recently, primary complexes of anilines with a deeply embedded adamantane subunit were reported.[33] The mentioned result suggests that the structure of the complexes between adamantane-based compounds and cyclodextrin could be strongly influenced by the substituents on the AMA subunit. Moreover, it indicates that the larger stability of the majority of secondary with respect to corresponding primary complexes cannot be solely explained by the truncated cone shape of the macrocycle. The crystal structure of the host and recent all atom molecular dynamics (MD) simulations of β-CD in explicit water supported this conclusion, since no considerable difference in the diameters of primary and secondary rim was observed in either case.[34,35]

In the present paper the 1:1 inclusion complexes **10**β·CD were formed by translation of the guest molecule through the CD cavity, entering via the secondary and primary rim, respectively (Fig. 6). The glycosidic oxygen atoms of CD were placed in the *xy*-plane and the corresponding centroid was defined as the origin of the coordinate system. The guest was allowed to approach the host along the *z*-axis coinciding with N–C (adamantamine) bond in the increments of 1 Å, defined by the distances between the centroid and one of the atoms connected by a bond (arbitrarily chosen N). Two directions of insertion for each orientation of glycoconjugate relative to CD were possible. The examined glycoconjugate hence faced the primary and the secondary rim of macrocycle with adamantane and with mannose subunit, respectively. The 1:1 inclusion complexes and host molecules were further optimized according to method described in the chapter Computational details.

The geometry of CD was optimized starting from the X-ray determined structure, with water molecules excluded according to the procedure described in the literature.[17,22,34] The obtained structure (**H2**) is shown in Fig. 7. The other, energetically more favourable conformer, (**H1**) is the result of conformational analysis. The notably smaller energy of the conformer **H1** with respect to **H2** can be attributed to formation of favourable hydrogen bonds between the facing C6 hydroxyl groups at the primary rim. As a consequence of realized hydrogen bonds the structure of cyclodextrin and corresponding cross section of its cavity changed from rounded (**H2**) to more elliptical shape (**H1**).

The structures of the selected **10**β·CD complexes (**M1**–**M5**), formed out of one guest (**10**β) and one host molecule (CD), and the corresponding relative energies can be seen in Figs. 8 and 9. The energetically most favourable complex **M1** is of slightly bent structure with adamantyl subunit situated within the cavity and the chiral linker passing through the primary rim of CD (i.e., primary complex). The complexes **M2**–**M5** with guest molecule

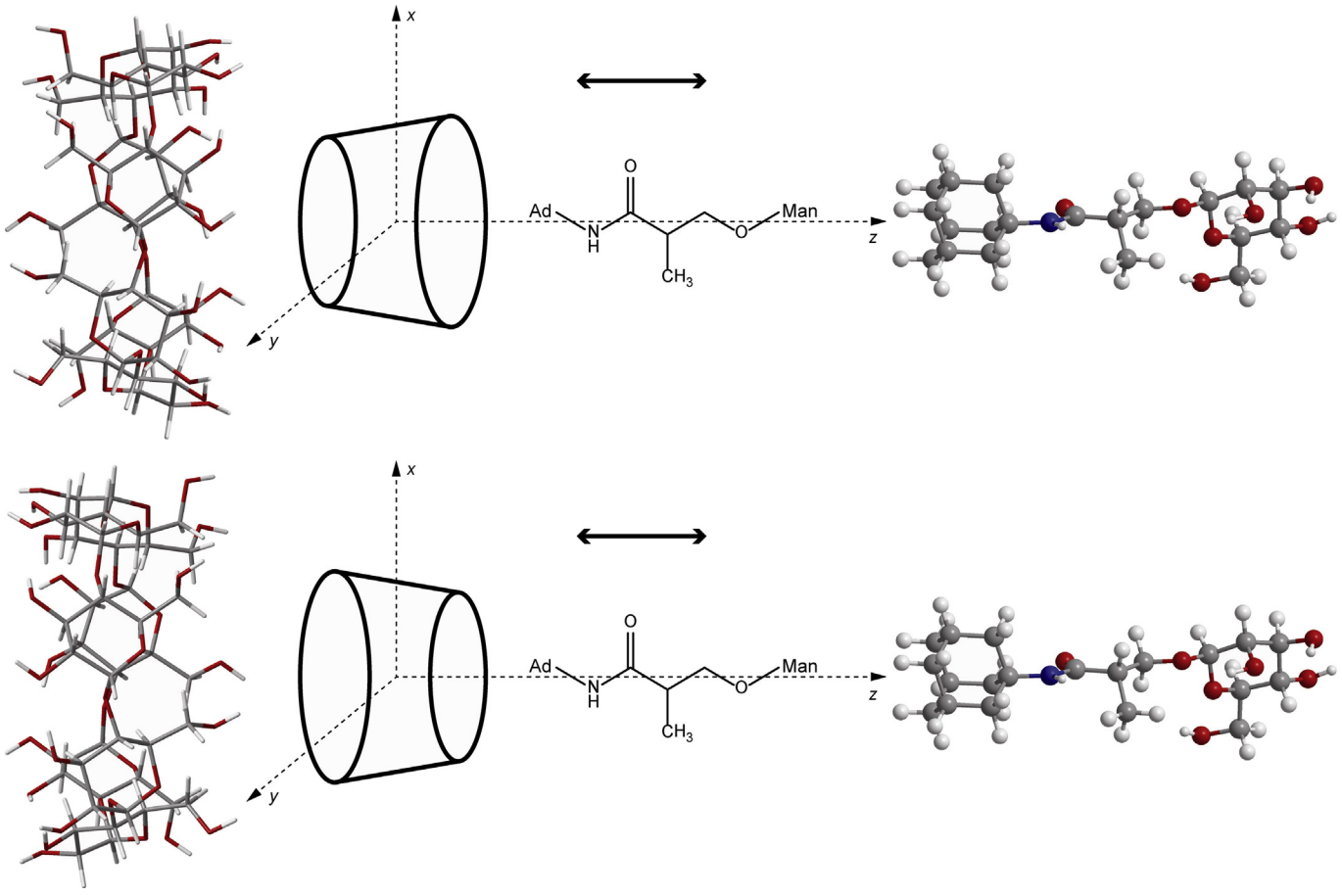

Fig. 6. The relative position of the guest (**10**β) and the host (CD) molecule in **10**β·CD complexes.

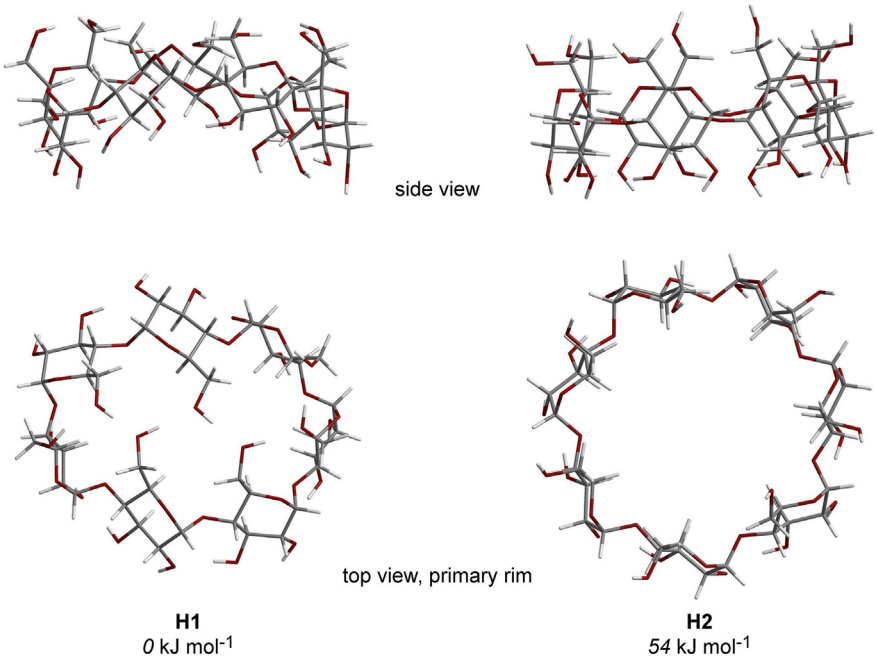

Fig. 7. B3LYP/6-31G(d) in water (PCM) optimized geometries of host (**H**) molecules. Relative energies of the selected CD are written in italic.

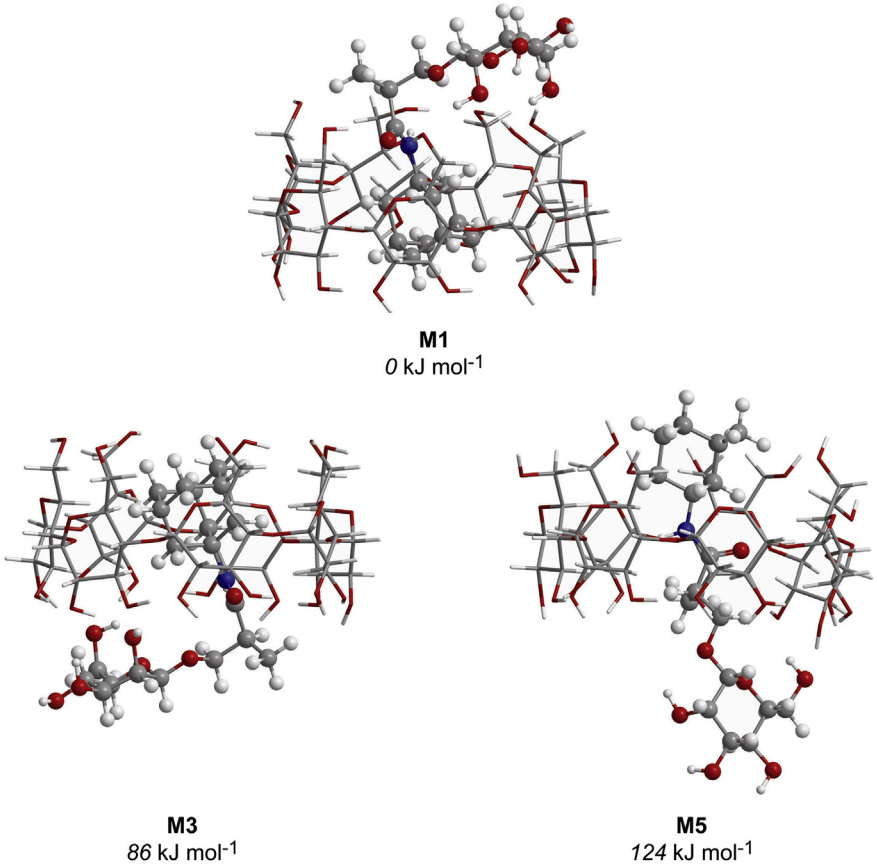

Fig. 8. Side view of B3LYP/6-31G(d) in water (PCM) optimized geometries of **10**β·CD inclusion complexes (**M1**, **M3** and **M5**). Relative energies of the complexes are written in italic.

protruding out of the secondary rim of CD are energetically less favourable.

According to the obtained results, the formation of hydrogen bonds between the guest molecules and CD significantly contributes to the overall stabilization of the inclusion complexes. This is most evident from the structures of the secondary complexes, **M3** and **M5**. As can be seen in Fig. 8, the pre-defined entrance orientation of the mannose conjugate is largely preserved in **M5**, resulting in weak participation of the sugar subunit in the complexation process. On the other hand, due to a slightly bent

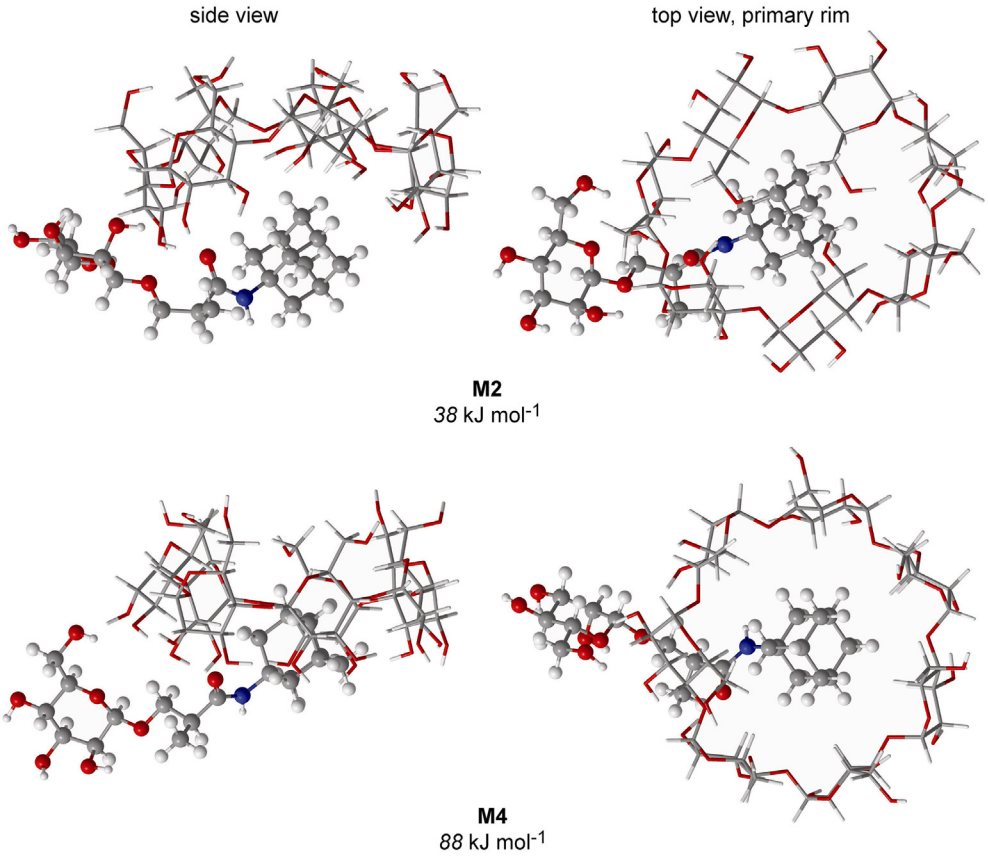

Fig. 9. Side and top view of B3LYP/6-31G(d) in water (PCM) optimized geometries of **10**β·CD inclusion complexes (**M2** and **M4**). Relative energies of the complexes are written in italic.

structure of the guest, the multiple hydrogen bonds of the hydrophilic part of the guest molecule and CD are realized in the conformer **M3**.

In order to explain the differences in the stability of the primary and secondary complexes, the hydrogen bond patterns in **M1** and **M3** (Fig. 10) were studied in detail by using Bader's atoms-in-molecules (AIM) theory,[36] which was reported as useful in the analysis of these interactions.[37,38] These two complexes were chosen for comparison due to the relatively similar conformation of the guest molecule. In the complex **M1** hydrogen bonding occurs at both rims of CD. At the primary rim of the macrocycle hydrogen bond donors and acceptors of guest molecule (−NH and C═O from chiral spacer and mannose −OH groups) form a ring with primary −OH groups of CD (eight hydrogen bonds in total). At the secondary rim seven O−H···O interactions between C2 and C3 hydroxyl groups of adjacent glucose units form a ring of hydrogen bonds. By contrast, the hydrogen bonds between the host and guest molecules in the **M3** complex are predominantly formed at the secondary rim. The hydrogen bonding pattern is comprised of seven O−H···O interactions between C2 and C3 hydroxyl groups. In this case, only mannose −OH groups, and not −HN and C═O groups of chiral linker, act as additional hydrogen bond donors and acceptors in interaction with secondary rim −OH groups. It should be noted that all hydrogen bonds occurring in the complexes **M1** and **M3** were verified using the AIM method according to Koch and Popelier formalism.[37,38]

Interestingly, the cross section of CD cavity is rather similar in **M1** and **M3** complexes. It resembles the rounded shape of **H2** conformer of the host. The computational investigations are hence in accord with the earlier investigations of the host structure,[34,35] which suggest that the difference between the diameters of the primary and the secondary rim is rather small. It is worth emphasizing that the energy of the conformer **M4** is quite similar to **M3**, even though the geometry of the complexes is quite different. The guest molecule in **M4** is not bent as in the case of **M3**, but rather tilted from the predefined entrance line. This, in turn, resulted in partial inclusion of the adamantyl subunit and only peripheral interactions of hydrophilic part of guest molecule with secondary −OH groups of CD.

Further reorganization of the CD structure from rounded (**M4**) to elliptical shape (**M2**) exposes the adamantyl subunit even more to the outer region. The lower energy of **M2** in comparison to **M4** is mostly the outcome of hydrogen bonds formation between the facing C6−OH groups at the primary rim of CD. The relative energy difference of **H2** and **H1** (54 kJ mol^{-1}) is almost identical to the corresponding difference of **M4** and **M2** complexes.

The appropriate modelling of solvent effects in the system studied is obviously very important. While favourable hydrogen bonds of the guest could be explicitly modelled with −OH groups of CD, the similar approach in modelling of water molecules is not possible due to their number. Therefore, a polarizable continuum model of the solvent (PCM) is usually used as the acceptable compromise between expensive computational time and adequate treatment of solvent effects. Another drawback of the implicit solvent model, in spite of its robustness, is inadequate treatment of the water molecules inside the cavity of CD.

Despite the fact that the computational findings are not in accord with experimental results, they do provide deeper insight into the complexation process. They indicate that the favourable solvation of hydrophilic part of the guest molecule might be significantly more pronounced in secondary complexes where the sugar part is positioned farther from the cavity of CD, due to the existence

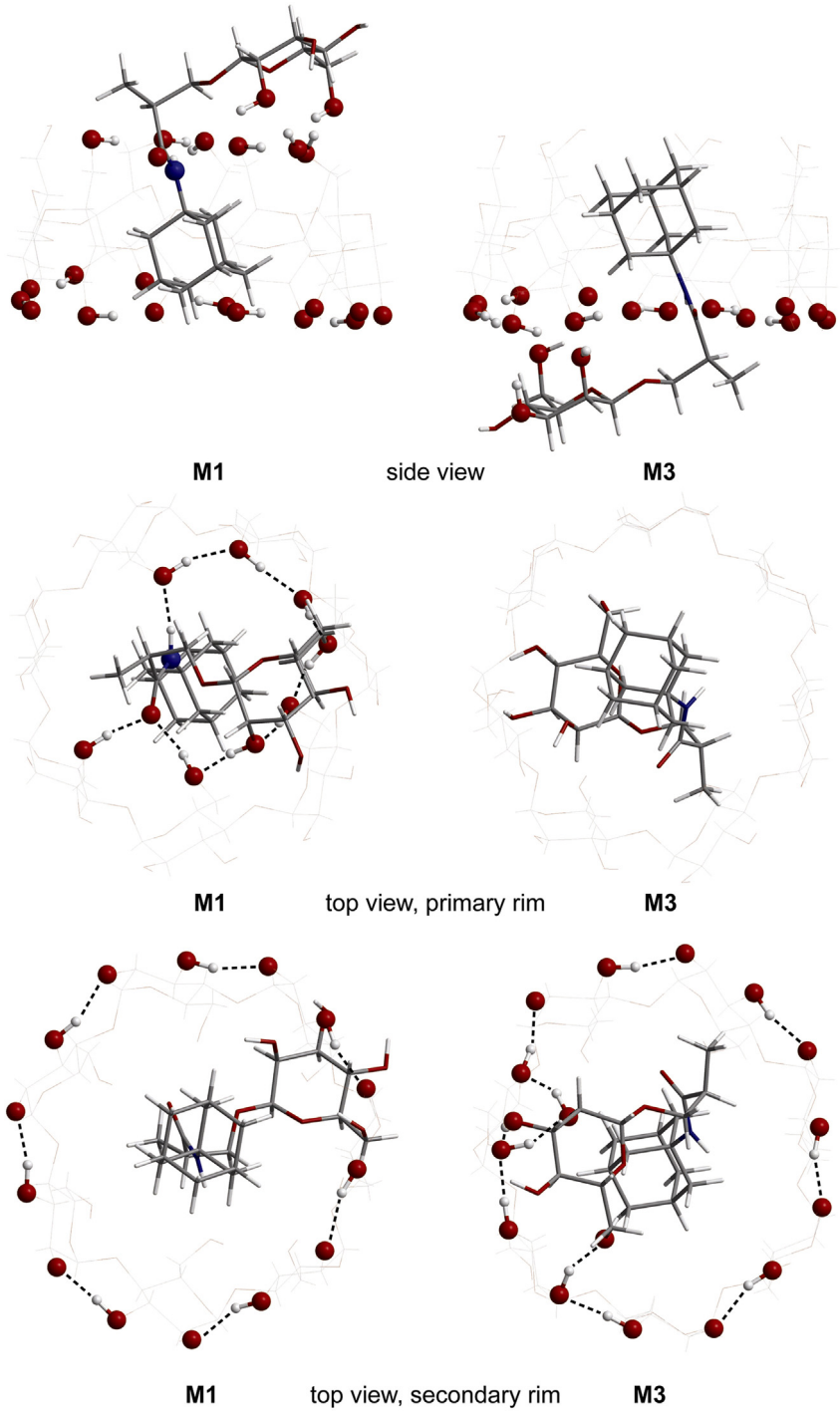

Fig. 10. Hydrogen bonds pattern at the primary and the secondary rim of B3LYP/6-31G(d) in water (PCM) optimized **10**β·CD inclusion complexes **M1** and **M3**.

of short secondary −OH, and not lengthy and more flexible primary $-CH_2OH$ groups. Consequently, the deep embedding of the AMA subunit with the hydrophilic part protruding out of the primary rim might require extensive dehydration of the hydrophilic part of the guest molecule than the formation of corresponding secondary complex. The majority of the literature data suggest that the formation of the secondary complexes is favoured due to the fact that the adamantane subunit does not fit into the primary rim of cyclodextrin. Our results indicate that this factor is perhaps less important for the explanation of the larger stability of secondary complexes with respect to the primary ones. As mentioned earlier, the formation of the primary complexes of AMA containing derivatives with cyclodextrin[33] and the crystal structure[34] of the macrocycle as well as MD simulations in explicit water[35] support these findings.

3. Conclusion

Comprehensive structural, thermodynamic and computational studies were undertaken in order to get a detailed insight into the binding of adamantyl glycoconjugates with β-CD. The experimental investigations included two series of glycosides, one with mannose and one with galactose sugar subunit. The synthesis of the latter series was reported here for the first time.

On the basis of the results of spectroscopic and microcalorimetric investigations it was concluded that 1:1 secondary complexes of the examined guests with β-CD are being formed, primarily as a result of adamantane inclusion into the hydrophobic cavity of the macrocycle. The NMR studies of adducts formed revealed the inclusion of adamantane subunit within the macrocycle and relatively weak involvement of the hydrophilic part of the guest molecules in the hosting process. The notably favourable complexation of the examined adamantyl glycosides (log $K \geq 4.5$) with β-CD is by large enthalpically controlled. The contribution of the standard reaction entropy to the binding energetics was favourable, but relatively small in the case of all investigated guests. The thermodynamically favourable hosting of examined ligands can be adequately explained by the hydrophobic hydration of the host cavity and the adamantane group on one hand and by the extensive hydration of both the linker functional groups and the sugar subunits covalently attached to the adamantane subunit on the other.

The computational studies support this conclusion—the notable preference for the formation of complexes and extensive hydrogen bonding between the host and the hydrophilic part of the guest molecule was noticed in the implicitly modelled water (PCM). According to those findings the reason for the difference in the stability of secondary and primary complexes could be dehydration of the hydrophilic subunit realized upon the complete inclusion of adamantane inside the cavity. The reason for this behaviour might be the fact that the presence of methylene groups at the primary rim pre-supposes more pronounced dehydration of the hydrophilic subunit of the guest than in the case of secondary complexes. Provided that the hydrophilic part of the guest experiences strong hydration (and hence remains largely solvated upon the adamantane inclusion) this could, at least partially, explain the experimentally observed larger stability of the secondary with respect to primary complexes of AMA based guests in water. The other reason might be the computationally observed difference in the hydrogen bonding pattern at the primary and the secondary rim of macrocycle. However, one should keep in mind that the applied theoretical model may exaggerate the tendency for the formation of hydrogen bonds between the primary hydroxyl groups.

4. Experimental

4.1. General methods for the synthesis of AMA galactoconjugates

Starting compound 2,3,4,6-tetra-*O*-benzyl-D-galactopyranosyl trichloroacetimidate was prepared according to the published procedure.[26] Linkers methyl (*R*)- and (*S*)-3-hydroxy-2-methylpropionates were purchased from Aldrich Corp. The other reagents used in syntheses were obtained from Aldrich Corp. and Fluka. All solvents were purified using the standard procedures. Column chromatography (solvents and proportions are given in text) was performed on Merck silica gel 60 (size 70–230 mesh ASTM) and TLC monitoring on Fluka silica gel (60F 254) plates (0.25 mm). Visualization was mostly achieved by the use of UV light and/or by charring with H_2SO_4. Optical rotations were measured at room temperature using the Schmidt+HaenschPolartronic NH8. ^1H and ^{13}C NMR spectra were recorded using Bruker Avance spectrometer with TMS as an internal standard. C, H and N analyses were provided by the Analytical Services Laboratory of RuđerBošković Institute, Zagreb.

4.2. Glycosylation of methyl (*R*)- and (*S*)-3-hydroxy-2-methylpropionates

Methyl (*R*)- or (*S*)-3-hydroxy-2-methylpropionate (151.1 μL, 1.37 mmol, 1.6 equiv) was suspended in dry DCM (2 mL) at 0 °C under N_2 and $BF_3 \cdot Et_2O$ was added (277.5 μL, 2.19 mmol, 1 equiv). Benzylated α,β-D-galactopyranosyltrichloroacetimidate (1.5 g, 2.19 mmol) suspended in dry DCM (2 mL) was then added dropwise within 15 min after which the reaction mixture was stirred for the additional 2.5 h and monitored by TLC (diethyl ether/petroleum ether 1:1). Iced 1 M $NaHCO_3$ was added and the resulting mixture was extracted with diethyl ether. Organic layers were washed with water and dried over Na_2SO_4. After filtration, the organic layer was concentrated in vacuo and the residue was purified by column chromatography on silica gel (diethyl ether/petroleum ether 1:1). The products were isolated as anomeric pale yellow oil mixtures (**1**α,β, 856 mg, 61%) and (**2**α,β, 912 mg, 65%). The anomeric mixtures were then rechromatographed to isolate the pure anomers of each ester derivative.

*4.2.1. Methyl (2R)-(2,3,4,6-tetra-O-benzyl-α-D-galactopyranosyloxy)-2-methylpropionate (**1**α).* Yellow oil; $[\alpha]_D$ +30.9 (*c* 0.56, $CHCl_3$); R_f (diethyl ether/petroleum ether 1:1)=0.39; ^1H NMR (300 MHz, $CDCl_3$) δ: 7.39–7.26 (m, 20H, H–Ar), 4.95 (d, J_{gem}=11.5 Hz, 1H, CH_2Ph), 4.87 (d, $J_{1,2}$=3.5 Hz, 1H, H-1), 4.86–4.64 (m, 4H, 2 CH_2Ph), 4.58 (d, J_{gem}=11.5 Hz, 1H, CH_2Ph), 4.51–4.39 (m, 2H, CH_2Ph), 4.04 (dd, $J_{1,2}$=3.8 Hz, $J_{2,3}$=10.13 Hz, 1H, H-2), 3.98–3.89 (m, 3H, H-3, H-4, H-5), 3.68–3.64 (m, 2H, H-6a, H-6b), 3.62 (s, 3H, OCH_3), 3.53 (d, *J*=6.4 Hz, 2H, OCH_2), 2.89–2.78 (m, 1H, CH), 1.19 (d, *J*=7.1 Hz, 3H, CH_3); ^{13}C NMR (75 MHz, $CDCl_3$) δ: 174.91 (C=O), 138.91, 138.82, 138.76, 138.13 (C–Ar), 128.37–127.33 (CH–Ar), 98.05 (C1), 78.87, 76.65, 75.23, 70.02 (C2–C5), 74.76, 73.47, 73.16, 72.86 ($4CH_2Ph$), 69.63 (C6), 69.06 (OCH_2), 51.59 (OCH_3), 39.95 (CH), 14.13 (CH_3). Anal. Calcd for $C_{39}H_{44}O_8$: C, 73.10; H, 6.92. Found: C, 73.02; H, 6.88.

*4.2.2. Methyl (2R)-(2,3,4,6-tetra-O-benzyl-β-D-galactopyranosyloxy)-2-methylpropionate (**1**β).* Yellow oil; $[\alpha]_D$ −13.7 (*c* 0.42, $CHCl_3$); R_f (diethyl ether/petroleum ether 1:1)=0.32; ^1H NMR (300 MHz, $CDCl_3$) δ: 7.37–7.25 (m, 20H, H–Ar), 4.93 (d, J_{gem}=11.7 Hz, 1H, CH_2Ph), 4.88–4.69 (m, 4H, $2CH_2Ph$), 4.62 (d, J_{gem}=11.7 Hz, 1H, CH_2Ph), 4.45–4.40 (m, 2H, CH_2Ph), 4.35 (d, $J_{1,2}$=7.7 Hz, 1H, H-1), 4.15–4.13 (m, 1H, H-3), 3.88 (d, $J_{4,5}$=2.6 Hz, 1H, H-4), 3.80 (dd, $J_{1,2}$=7.7 Hz, $J_{2,3}$=9.7 Hz, 1H, H-2), 3.61 (s, 3H, OCH_3), 3.60–3.50 (m, 5H, H-6a, H-6b, H-5, OCH_2), 2.83–2.77 (m, 1H, CH), 1.24 (d, *J*=7.1 Hz, 3H, CH_3); ^{13}C NMR (75 MHz, $CDCl_3$) δ: 174.76 (C=O), 138.68, 138.57, 138.47, 137.89 (C–Ar), 128.50–127.40 (CH–Ar), 104.14 (C1), 82.13, 79.30, 73.44, 73.44 (C2–C5), 75.07, 74.51, 73.52, 73.07 (CH_2Ph), 71.22 (C6), 68.74 (OCH_2), 51.69 (OCH_3), 40.04 (CH), 14.15 (CH_3). Anal. Calcd for $C_{39}H_{44}O_8$: C, 73.10; H, 6.92. Found: C, 72.88; H, 6.89.

*4.2.3. Methyl (2S)-(2,3,4,6-tetra-O-benzyl-α-D-galactopyranosyloxy)-2-methylpropionate (**2**α).* Yellow oil; $[\alpha]_D$ +24.2 (*c* 0.41, $CHCl_3$); R_f (diethyl ether/petroleum ether 1:1)=0.34; ^1H NMR (300 MHz, $CDCl_3$) δ: 7.36–7.25 (m, 20H, H–Ar), 4.95 (d, J_{gem}=11.44 Hz, 1H, CH_2Ph), 4.82 (d, $J_{1,2}$=3.8 Hz, 1H, H-1), 4.80–4.63 (m, 4H, 2 CH_2Ph), 4.56 (d, J_{gem}=11.4 Hz, 1H, CH_2Ph), 4.51–4.40 (m, 2H, CH_2Ph), 4.03 (dd, $J_{1,2}$=3.6 Hz, $J_{2,3}$=10.0 Hz, 1H, H-2), 4.00–3.85 (m, 4H, H-3, H-4, H-5, H-6a), 3.61 (s, 3H, OCH_3), 3.53 (d, *J*=6.5 Hz, 2H, OCH_2), 3.40 (dd, $J_{6a,5}$=5.9 Hz, $J_{6a,6b}$=9.6 Hz, 1H, H-6b), 2.89–2.75 (m, 1H, CH), 1.18 (d, *J*=7.1 Hz, 3H, CH_3); ^{13}C NMR (75 MHz, $CDCl_3$) δ: 175.02 (C=O), 138.83, 138.73, 138.70, 138.09 (C–Ar), 128.40–127.32 (CH–Ar), 97.84 (C1), 78.82, 76.54, 75.01, 69.36 (C2–C5), 74.74, 73.35, 73.06, 73.06 (CH_2Ph), 69.81 (C6), 68.83 (OCH_2), 51.62 (OCH_3), 39.79 (CH), 14.22 (CH_3). Anal. Calcd for $C_{39}H_{44}O_8$: C, 73.10; H, 6.92. Found: C, 73.01; H, 6.90.

*4.2.4. Methyl (2S)-(2,3,4,6-tetra-O-benzyl-β-D-galactopyranosyloxy)-2-methylpropionate (**2**β).* Yellow oil; $[\alpha]_D$ −20.1 (*c* 0.30, $CHCl_3$); R_f (diethyl ether/petroleum ether 1:1)=0.31; ^1H NMR (300 MHz, $CDCl_3$) δ: 7.38–7.25 (m, 20H, H–Ar), 4.92 (d, J_{gem}=11.6 Hz, 1H,

CH_2Ph), 4.88–4.66 (m, 4H, 2 CH_2Ph), 4.61 (d, J_{gem}=11.7 Hz, 1H, CH_2Ph), 4.47–4.38 (m, 2H, CH_2Ph), 4.35 (d, $J_{1,2}$=7.7 Hz, 1H, H-1), 3.94–3.87 (m, 2H, H-3, H-4), 3.81–3.70 (m, 2H, H-2, H-5), 3.59 (s, 3H, OCH_3), 3.61–3.47 (m, 4H, OCH_2, H-6a, H-6b), 2.87–2.75 (m, 1H, CH), 1.16 (d, J=7.2 Hz, 3H, CH_3); ^{13}C NMR (75 MHz, $CDCl_3$) δ: 175.27 (C=O), 138.71, 138.56, 138.49, 137.88 (C–Ar), 128.44–127.40 (CH–Ar), 104.03 (C1), 82.05, 79.25, 73.46, 73.39 (C2–C5), 74.90, 74.50, 73.51, 73.10 (4CH_2Ph), 71.39 (C6), 68.77 (OCH_2), 51.71 (OCH_3), 40.25 (CH), 14.09 (CH_3). Anal. Calcd for $C_{39}H_{44}O_8$: C, 73.10; H, 6.92. Found: C, 72.90; H, 6.86.

4.3. General procedure for methyl ester hydrolysis

To a solution of pure anomer of each ester derivative **1**α, **1**β, **2**α and **2**β (100 mg, 0.16 mmol) in dioxane (1 mL) 10 equiv of 1 M NaOH was added and the reaction mixture was stirred for 24 h at 40 °C and monitored by TLC (C_6H_6/EtOAc 2:1). Reaction mixtures were then treated with 0.5 M HCl (pH 3.5) and saturated brine was added. Mixtures were extracted with diethyl ether and organic layers dried over Na_2SO_4. After filtration, the organic layer was concentrated in vacuo and the residues purified by column chromatography on silica gel ($CHCl_3$/MeOH 9:1) and corresponding acids were isolated.

*4.3.1. (2R)-(2,3,4,6-Tetra-O-benzyl-α-D-galactopyranosyloxy)-2-methylpropionicacid(**3**α).* Pale yellow oil (80.2 mg, 82%); $[\alpha]_D$ +15.6 (*c* 0.42, $CHCl_3$); R_f ($CHCl_3$/CH_3OH 9:1)=0.66; ^{1}H NMR (300 MHz, $CDCl_3$) δ: 7.35–7.25 (m, 20H, H–Ar), 4.92 (d, J_{gem}=11.5 Hz, 1H, CH_2Ph), 4.81 (d, $J_{1,2}$=3.9 Hz, 1H, H-1), 4.78–4.64 (m, 4H, 2CH_2Ph), 4.55 (d, J_{gem}=11.5 Hz, 1H, CH_2Ph), 4.49–4.37 (m, 2H, CH_2Ph), 4.03 (dd, $J_{1,2}$=3.7 Hz, $J_{2,3}$=9.9 Hz, 1H, H-2), 3.94–3.87 (m, 3H, H-3, H-4, H-5), 3.69 (dd, $J_{6a,5}$=5.8 Hz, $J_{6a,6b}$=9.9 Hz, 1H, H-6a), 3.63–3.50 (m, 3H, H-6b, OCH_2), 2.85–2.74 (m, 1H, CH), 1.17 (d, J=7.1 Hz, 3H, CH_3); ^{13}C NMR (75 MHz, $CDCl_3$) δ: 177.89 (C=O), 138.65, 138.51, 138.37, 137.82 (C–Ar), 128.45–127.38 (CH–Ar), 98.46 (C1), 78.86, 76.11, 74.84, 69.76 (C2–C5), 74.71, 73.50, 73.28, 73.10 (CH_2Ph), 70.02 (C6), 69.07 (OCH_2), 39.45 (CH), 13.59 (CH_3). Anal. Calcd for $C_{38}H_{42}O_8$: C, 72.82; H, 6.75. Found: C, 72.60; H, 6.65.

*4.3.2. (2R)-(2,3,4,6-Tetra-O-benzyl-β-D-galactopyranosyloxy)-2-methylpropionic acid (**3**β).* Pale yellow oil (77.2 mg, 79%); $[\alpha]_D$ −15.5 (*c* 0.46, $CHCl_3$); R_f ($CHCl_3$/CH_3OH 9:1)=0.53; ^{1}H NMR (300 MHz, $CDCl_3$) δ: 7.36–7.22 (m, 20H, H–Ar), 4.89 (d, J_{gem}=11.5 Hz, 1H, CH_2Ph), 4.84–4.62 (m, 4H, 2CH_2Ph), 4.57 (d, J_{gem}=11.7 Hz, 1H, CH_2Ph), 4.49–4.39 (m, 2H, CH_2Ph), 4.36 (d, $J_{1,2}$=7.7 Hz, 1H, H-1), 4.14–4.09 (m, 1H, H-3), 3.78 (dd, $J_{1,2}$=7.9 Hz, $J_{2,3}$=9.8 Hz, 1H, H-2), 3.74 (d, $J_{4,5}$=2.7 Hz, 1H, H-4), 3.68–3.45 (m, 5H, OCH_2, H-6a, H-6b, H-5), 2.84–2.72 (m, 1H, CH), 1.24 (d, J=7.2 Hz, 3H, CH_3); ^{13}C NMR (75 MHz, $CDCl_3$) δ: 178.64 (C=O), 138.60, 138.43, 138.43, 137.62 (C–Ar), 128.43–127.38 (CH–Ar), 104.06 (C1), 82.11, 79.34, 73.42, 73.15 (C2–C5), 75.19, 74.38, 73.50, 72.97 (CH_2Ph), 71.03 (C6), 68.98 (OCH_2), 39.83 (CH), 13.80 (CH_3). Anal. Calcd for $C_{38}H_{42}O_8$: C, 72.82; H 6.75. Found: C, 72.64; H, 6.60.

*4.3.3. (2S)-(2,3,4,6-Tetra-O-benzyl-α-D-galactopyranosyloxy)-2-methylpropionic acid (**4**α).* Pale yellow oil (82.1 mg, 84%); $[\alpha]_D$ +34.5 (*c* 0.82, $CHCl_3$); R_f ($CHCl_3$/CH_3OH 9:1)=0.70; ^{1}H NMR (300 MHz, $CDCl_3$) δ: 7.38–7.24 (m, 20H, H–Ar), 4.91 (d, J_{gem}=11.4 Hz, 1H, CH_2Ph), 4.79 (d, $J_{1,2}$=3.4 Hz, 1H, H-1), 4.77–4.64 (m, 4H, 2 CH_2Ph), 4.54 (d, J_{gem}=11.4 Hz, 1H, CH_2Ph), 4.50–4.37 (m, 2H, CH_2Ph), 4.04 (dd, $J_{1,2}$=3.6 Hz, $J_{2,3}$=9.9 Hz, 1H, H-2), 3.97–3.80 (m, 4H, H-3, H-4, H-5, H-6a), 3.51 (d, J=6.1 Hz, 2H, OCH_2), 3.46 (dd, $J_{6b,5}$=5.4 Hz, $J_{6a,6b}$=10.1 Hz, 1H, H-6b), 2.81–2.70 (m, 1H, CH), 1.17 (d, J=7.1 Hz, 3H, CH_3); ^{13}C NMR (75 MHz, $CDCl_3$) δ: 178.00 (C=O), 138.60, 138.52, 138.23, 137.87 (C–Ar), 128.48–127.34 (CH–Ar), 97.96 (C1), 78.85, 76.25, 74.83, 69.60 (C2–C5), 74.73, 73.52, 73.37, 72.96 (CH_2Ph), 69.63 (C6), 68.87 (OCH_2), 39.47 (CH), 13.72 (CH_3). Anal. Calcd for $C_{38}H_{42}O_8$: C, 72.82; H, 6.75. Found: C, 72.59; H, 6.67.

*4.3.4. (2S)-(2,3,4,6-Tetra-O-benzyl-β-D-galactopyranosyloxy)-2-methylpropionic acid (**4**β).* Pale yellow oil (80.2 mg, 82%); $[\alpha]_D$ −4.5 (*c* 0.76, $CHCl_3$); R_f ($CHCl_3$/CH_3OH 9:1)=0.59; ^{1}H NMR (300 MHz, $CDCl_3$) δ: 7.33–7.21 (m, 20H, H–Ar), 4.89 (d, J_{gem}=11.7 Hz, 1H, CH_2Ph), 4.86–4.62 (m, 4H, 2CH_2Ph), 4.57 (d, J_{gem}=11.7 Hz, 1H, CH_2Ph), 4.49–4.42 (m, 2H, CH_2Ph), 4.37 (d, $J_{1,2}$=7.8 Hz, 1H, H-1), 3.95–3.90 (m, 1H, H-3), 3.80–3.70 (m, 3H, H-2, H-4, H-5), 3.60–3.46 (m, 4H, OCH_2, H-6a, H-6b), 2.85–2.74 (m, 1H, CH), 1.17 (d, J=7.1 Hz, 3H, CH_3); ^{13}C NMR (75 MHz, $CDCl_3$) δ: 178.51 (C=O), 138.55, 138.42, 138.39, 137.68 (C–Ar), 128.46–127.41 (CH–Ar), 104.04 (C1), 82.03, 79.23, 73.45, 73.30 (C2–C5), 75.11, 74.45, 73.52, 73.04 (CH_2Ph), 71.37 (C6), 68.86 (OCH_2), 40.08 (CH), 13.78 (CH_3). Anal. Calcd for $C_{38}H_{42}O_8$: C, 72.82; H, 6.75. Found: C, 72.65; H, 6.62.

4.4. General procedure for the synthesis of AMA glycoconjugates

To a solution of pure anomer of each carboxylic acid derivative **3**α, **3**β, **4**α and **4**β (100 mg, 0.16 mmol) in dry DCM at 0 °C, EDC·HCl (25.4 mg, 0.21 mmol, 1.3 equiv) previously mixed with Et_3N (28.8 μL) was added. The mixtures were then stirred for 0.5 h at the same temperature. HOBt·H_2O (21.6 mg, 0.16 mmol, 1 equiv) was added next and the mixtures were left stirring for additional 2 h. During that time the reaction mixture was allowed to gradually reach the room temperature. AMA·HCl (150.1 mg, 0.8 mmol) previously mixed with Et_3N (110.9 μL) was then added and the reaction mixtures were left stirring overnight. After treatment with 0.5 M HCl (pH 3.5) the mixtures were extracted with DCM, the combined organic layers were washed with saturated $NaHCO_3$ and dried over Na_2SO_4. After the filtration, the organic layers were concentrated in vacuo and the residues purified by column chromatography on silica gel (C_6H_6/EtOAc 2:1) followed by the isolation of AMA glycoconjugates.

*4.4.1. (2R)-N-(Adamant-1-yl)-3-(2,3,4,6-tetra-O-benzyl-α-D-galacto pyranosyloxy)-2-methylpropanamide (**5**α).* Pale yellow oil (68.1 mg, 56%); $[\alpha]_D$ +10.6 (*c* 0.72, $CHCl_3$); R_f (C_6H_6/EtOAc 2:1)=0.64; ^{1}H NMR (300 MHz, $CDCl_3$) δ: 7.39–7.25 (m, 20H, H–Ar), 5.96 (s, 1H, N–H), 4.96 (d, J_{gem}=11.1 Hz, 1H, CH_2Ph), 4.84 (d, $J_{1,2}$=3.7 Hz, 1H, H-1), 4.81–4.66 (m, 4H, 2CH_2Ph), 4.58 (d, J_{gem}=11.5 Hz, 1H, CH_2Ph), 4.51–4.37 (m, 2H, CH_2Ph), 4.04 (dd, $J_{1,2}$=3.6 Hz, $J_{2,3}$=9.9 Hz, 1H, H-2), 3.97 (app t, J=6.4 Hz, J=6.5 Hz, 1H, H-5), 3.93–3.87 (m, 2H, H-3, H-4), 3.68–3.44 (m, 4H, H-6a, H-6b, OCH_2), 2.54–2.43 (m, 1H, CH), 1.96 (s, 3H, 3Hβ–AMA), 1.89 (s, 6H, 3Hα–AMA), 1.59 (s, 6H, 3Hγ–AMA), 1.06 (d, J=7.1 Hz, 3H, CH_3); ^{13}C NMR (75 MHz, $CDCl_3$) δ: 173.47 (C=O), 138.70, 138.56, 138.54, 137.76 (C–Ar), 128.35–127.38 (CH–Ar), 98.78 (C1), 79.02, 76.43, 75.19, 69.70 (C2–C5), 74.71, 73.60, 73.22, 73.18 (CH_2Ph), 71.46 (C6), 69.44 (OCH_2), 51.48 (C–N), 41.73 (CH), 41.49 (Cα–AMA), 36.34 (Cγ–AMA), 29.38 (Cβ–AMA), 14.33 (CH_3). Anal. Calcd for $C_{48}H_{57}NO_7$: C, 75.86; H, 7.56; N, 1.84. Found: C, 75.69; H, 7.60; N, 1.89.

*4.4.2. (2R)-N-(Adamant-1-yl)-3-(2,3,4,6-tetra-O-benzyl-β-D-galactopyranosyloxy)-2-methylpropanamide (**5**β).* Pale yellow oil (67.0 mg, 55%); $[\alpha]_D$ −7.3 (*c* 0.66, $CHCl_3$); R_f (C_6H_6/EtOAc 2:1)=0.53; ^{1}H NMR (300 MHz, $CDCl_3$) δ: 7.36–7.25 (m, 20H, H–Ar), 5.76 (br s, 1H, N–H), 4.94 (d, J_{gem}=11.6 Hz, 1H, CH_2Ph), 4.90–4.73 (m, 4H, 2 CH_2Ph), 4.58 (d, J_{gem}=11.6 Hz, 1H, CH_2Ph), 4.48–4.39 (m, 2H, CH_2Ph), 4.35 (d, $J_{1,2}$=7.6 Hz, 1H, H-1), 4.00–3.94 (m,1H, H-3), 3.90 (d, $J_{4,5}$=2.8 Hz, 1H, H-4), 3.78 (dd, $J_{1,2}$=7.7 Hz, $J_{2,3}$=9.7 Hz, 1H, H-2), 3.60–3.48 (m, 5H, H-5, H-6a, H-6b, OCH_2), 2.50–2.39 (m, 1H, CH), 1.96 (s, 3H, 3Hβ–AMA), 1.92 (s, 6H, 3Hα–AMA), 1.60 (s, 6H, 3Hγ–AMA), 1.12 (d, J=7.1 Hz, 3H, CH_3); ^{13}C NMR (75 MHz, $CDCl_3$) δ: 173.08 (C=O),

138.70, 138.63, 138.37, 137.77 (C–Ar), 128.44–127.46 (CH–Ar), 103.44 (C1), 82.17, 79.42, 73.56, 73.39 (C2–C5), 75.18, 74.59, 73.58, 72.95 (CH_2Ph), 71.64 (C6), 68.59 (OCH_2), 51.59 (C–N), 41.45 (Cα–AMA), 41.42 (CH), 36.38 (Cγ–AMA), 29.39 (Cβ–AMA), 14.06 (CH_3). Anal. Calcd for $C_{48}H_{57}NO_7$: C, 75.86; H, 7.56; N, 1.84. Found: C, 75.72; H, 7.57; N, 1.92.

*4.4.3. (2S)-N-(Adamant-1-yl)-3-(2,3,4,6-tetra-O-benzyl-α-D-galacto pyranosyloxy)-2-methylpropanamide (**6**α).* Pale yellow oil (80.2 mg, 66%); $[\alpha]_D$ +31.8 (*c* 0.40, $CHCl_3$); R_f (C_6H_6/EtOAc 2:1)=0.53; ^{1}H NMR (300 MHz, $CDCl_3$) δ: 7.37–7.25 (m, 20H, H–Ar), 6.09 (s, 1H, N–H), 4.94 (d, J_{gem}=11.4 Hz, 1H, CH_2Ph), 4.73 (d, $J_{1,2}$=3.4 Hz, 1H, H-1), 4.81–4.65 (m, 4H, $2CH_2Ph$), 4.58 (d, J_{gem}=11.4 Hz, 1H, CH_2Ph), 4.53–4.39 (m, 2H, CH_2Ph), 4.05 (dd, $J_{1,2}$=3.5 Hz, $J_{2,3}$=10.1 Hz, 1H, H-2), 4.00–3.89 (m, 3H, H-3, H-4, H-5), 3.74–3.37 (m, 4H, H-6a, H-6b, OCH_2), 2.45–2.38 (m, 1H, CH), 1.96 (s, 3H, 3Hβ–AMA), 1.89 (s, 6H, 3Hα–AMA), 1.59 (s, 6H, 3Hγ–AMA), 1.05 (d, *J*=7.0 Hz, 3H, CH_3); ^{13}C NMR (75 MHz, $CDCl_3$) δ: 173.57 (C=O), 138.61, 138.61, 138.29, 138.03 (C–Ar), 128.39–127.25 (CH–Ar), 97.85 (C1), 79.28, 76.40, 74.88, 69.38 (C2–C5), 74.85, 73.88, 73.32, 72.92 (CH_2Ph), 70.60 (C6), 68.54 (OCH_2), 51.55 (C–N), 41.51 (Cα–AMA), 41.07 (CH), 36.36 (Cγ–AMA), 29.39 (Cβ–AMA), 13.67 (CH_3). Anal. Calcd for $C_{48}H_{57}NO_7$: C, 75.86; H, 7.56; N, 1.84. Found: C, 75.68; H, 7.62; N, 1.93.

*4.4.4. (2S)-N-(Adamant-1-yl)-3-(2,3,4,6-tetra-O-benzyl-β-D-galactopyranosyloxy)-2-methylpropanamide (**6**β).* Pale yellow oil (73.0 mg, 60%); $[\alpha]_D$ +16.3 (*c* 0.82, $CHCl_3$); R_f (C_6H_6/EtOAc 2:1)=0.45; ^{1}H NMR (300 MHz, $CDCl_3$) δ: 7.37–7.25 (m, 20H, H–Ar), 5.90 (br s, 1H, N–H), 4.94 (d, J_{gem}=11.5 Hz, 1H, CH_2Ph), 4.90–4.69 (m, 4H, $2CH_2Ph$), 4.57 (d, J_{gem}=11.6 Hz, 1H, CH_2Ph), 4.44 (br s, 2H, CH_2Ph), 4.37 (d, $J_{1,2}$=6.6 Hz, 1H, H-1), 3.88–3.69 (m, 4H, H-2, H-3, H-4, H-5), 3.61–3.49 (m, 4H, OCH_2, H-6a, H-6b), 2.58–2.48 (m, 1H, CH), 1.98 (s, 3H, 3Hβ–AMA), 1.91 (s, 6H, 3Hα–AMA), 1.57 (s, 6H, 3Hγ–AMA), 1.05 (d, *J*=6.9 Hz, 3H, CH_3); ^{13}C NMR (75 MHz, $CDCl_3$) δ: 173.77 (C=O), 138.62, 138.58, 138.40, 137.68 (C–Ar), 128.52–127.46 (CH–Ar), 104.76 (C1), 81.97, 79.43, 73.73, 73.36 (C2–C5), 75.14, 74.65, 73.58, 73.10 (CH_2Ph), 73.00 (C6), 68.82 (OCH_2), 51.60 (C–N), 42.19 (CH), 41.47 (Cα–AMA), 36.37 (Cγ–AMA), 29.36 (Cβ–AMA), 13.89 (CH_3). Anal. Calcd for $C_{48}H_{57}NO_7$: C, 75.86; H, 7.56; N, 1.84. Found: C, 75.70; H, 7.59; N, 1.90.

4.5. General procedure for debenzylation of AMA conjugates

To a solution of pure anomer of each AMA conjugate **5**α, **5**β, **6**α and **6**β (100 mg, 0.13 mmol) in DCM (5 mL) 50 mg of 10% Pd/C and 20 mL of CH_3OH was added. The mixtures were subjected to hydrogen atmosphere under 4 bar at room temperature while being stirred for 24 h. The mixtures were then filtered over a Celite bed and the obtained filtrates were concentrated in vacuo. The residues were purified by column chromatography on silica gel (CH_3CN/H_2O 5:1) and deprotected compounds were obtained.

*4.5.1. (2R)-N-(Adamant-1-yl)-3-α-D-galactopyranosyloxy-2-methylpropanamide (**7**α).* Pale yellow crude foam (50.1 mg, 95%); $[\alpha]_D$ +54.2 (*c* 0.50, CH_3OH); R_f (CH_3CN/H_2O 5:1)=0.56; ^{1}H NMR (300 MHz, CD_3OD) δ: 4.87 (s, 1H, N–H), 4.81 (d, $J_{1,2}$=3.2 Hz, 1H, H-1), 3.87–3.65 (m, 6H, H-2, H-3, H-4, H-5, H-6a, H-6b), 3.61 (d, *J*=6.8 Hz, 2H, OCH_2), 2.71–2.60 (m, 1H, CH), 2.04 (br s, 9H, 3Hβ–AMA, 3Hα–AMA), 1.70 (s, 6H, 3Hγ–AMA), 1.05 (d, *J*=7.0 Hz, 3H, CH_3); ^{13}C NMR (75 MHz, CD_3OD) δ: 176.76 (C=O), 101.21 (C1), 72.58, 71.74, 71.15, 70.38 (C2–C5), 72.20 (C6), 62.90 (OCH_2), 52.88 (C–N), 42.78 (CH), 42.36 (Cα–AMA), 37.54 (Cγ–AMA), 30.95 (Cβ–AMA), 14.87 (CH_3). Anal. Calcd for $C_{20}H_{33}NO_7$: C, 60.13; H, 8.33; N, 3.51. Found: C, 60.01; H, 8.25; N, 3.32.

*4.5.2. (2R)-N-(Adamant-1-yl)-3-β-D-galactopyranosyloxy-2-methylpropanamide (**7**β).* Pale yellow crude foam (49.6 mg, 94%); $[\alpha]_D$ −18.1 (*c* 0.62, CH_3OH); R_f (CH_3CN/H_2O 5:1)=0.54; ^{1}H NMR (300 MHz, CD_3OD) δ: 7.23 (br s, 1H, N–H), 4.23 (d, $J_{1,2}$=7.06 Hz, 1H, H-1), 3.98–3.92 (m, 1H, H-3), 3.83 (d, $J_{4,5}$=2.8 Hz, 1H, H-4), 3.80–3.68 (m, 2H, H-2, H-5), 3.52–3.45 (m, 4H, H-6a, H-6b, OCH_2), 2.67–2.55 (m, 1H, CH), 2.03 (s, 9H, 3Hβ–AMA, 3Hα–AMA), 1.71 (s, 6H, 3Hγ–AMA), 1.07 (d, *J*=7.0 Hz, 3H, CH_3); ^{13}C NMR (75 MHz, CD_3OD) δ: 176.72 (C=O), 104.84 (C1), 76.72, 75.02, 72.40, 70.41 (C2–C5), 72.57 (C6), 62.57 (OCH_2), 52.90 (C–N), 42.54 (CH), 42.37 (Cα–AMA), 37.55 (Cγ–AMA), 30.94 (Cβ–AMA), 14.73 (CH_3). Anal. Calcd for $C_{20}H_{33}NO_7$: C, 60.13; H, 8.33; N, 3.51. Found: C, 60.07; H, 8.22; N, 3.29.

*4.5.3. (2S)-N-(Adamant-1-yl)-3-α-D-galactopyranosyloxy-2-methylpropanamide (**8**α).* Pale yellow crude foam (49.0 mg, 93%); $[\alpha]_D$ +131.8 (*c* 0.44, CH_3OH); R_f (CH_3CN/H_2O5:1)=0.56; ^{1}H NMR (300 MHz, CD_3OD) δ: 7.32 (br s, 1H, N–H), 4.77 (d, $J_{1,2}$=3.3 Hz, 1H, H-1), 3.85–3.83 (m, 1H, H-2), 3.80–3.64 (m, 6H, H-3, H-4, H-5, H-6a, OCH_2), 3.25 (dd, $J_{6a,5}$=4.6 Hz, $J_{6a,6b}$=9.2 Hz, 1H, H-6b), 2.69–2.56 (m, 1H, CH), 2.08 (br s, 9H, 3Hβ–AMA, 3Hα–AMA), 1.70 (s, 6H, 3Hγ–AMA), 1.02 (d, *J*=7.0 Hz, 3H, CH_3); ^{13}C NMR (75 MHz, CD_3OD) δ: 176.82 (C=O), 100.08 (C1), 72.14, 71.67, 71.07, 70.17 (C2–C5), 71.04 (C6), 62.74 (OCH_2), 52.87 (C–N), 42.50 (Cα–AMA), 42.40 (CH), 37.54 (Cγ–AMA), 30.95 (CH–AMA), 14.33 (CH_3). Anal. Calcd for $C_{20}H_{33}NO_7$: C, 60.13; H, 8.33; N, 3.51. Found: C, 60.02; H, 8.30; N, 3.35.

*4.5.4. (2S)-N-(Adamant-1-yl)-3-β-D-galactopyranosyloxy-2-methylpropanamide (**8**β).* Pale yellow crude foam (48.0 mg, 91%); $[\alpha]_D$ +24.4 (*c* 0.57, CH_3OH); R_f (CH_3CN/H_2O 5:1)=0.55; ^{1}H NMR (300 MHz, CD_3OD) δ: 4.84 (s, 1H, N–H), 4.21 (d, $J_{1,2}$=7.5 Hz, 1H, H-1), 3.82–3.68 (m, 5H, H-2, H-3, H-4, H-5, H-6a), 3.52–3.45 (m, 3H, H-6b, OCH_2), 2.66–2.61 (m, 1H, CH), 2.04 (s, 9H, 3Hβ–AMA, 3Hα–AMA), 1.71 (s, 6H, 3Hγ–AMA), 1.03 (d, *J*=7.0 Hz, 3H, CH_3); ^{13}C NMR (75 MHz, CD_3OD) δ: 176.81 (C=O), 105.59 (C1), 76.80, 74.96, 72.64, 70.31 (C2–C5), 73.48 (C6), 62.58 (OCH_2), 52.85 (C–N), 42.97 (CH), 42.35 (Cα–AMA), 37.58 (Cγ–AMA), 30.98 (Cβ–AMA), 14.59 (CH_3). Anal. Calcd for $C_{20}H_{33}NO_7$: C, 60.13; H, 8.33; N, 3.51. Found: C, 59.98; H, 8.26; N, 3.30.

4.6. NMR investigations

The ^{1}H NMR investigations of the hosting process were performed by means of Bruker Avance (600 MHz) spectrometer at 25 °C. For that purpose solutions containing pure and mixed reactants were prepared in 99.96% D_2O. The corresponding spectra were recorded and the chemical shifts of the reaction participants were referenced to internal D_2O (δ=4.80 ppm). ^{1}H NMR titration of **11**β with cyclodextrin was performed by adding aliquots of the stock host solution to the guest solutions up to 1:2 guest to host molar ratio. The guest concentration (*c*=1 mM) was kept constant in all cases and the concentration of macrocycle was varied.

For all the other examined galactose and mannose conjugates only the ^{1}H NMR spectra of the solution at the 1:2 guest to host molar ratio were collected. For that purpose, the host solution (*c*=20 M) was added to the guest solution (*c*=5 mM). The ROESY spectra of the reaction mixtures at 1:1 guest to host molar ratio were recorded in the case of **10**α and **10**β derivatives.

4.7. Microcalorimetry

Microcalorimetric experiments were performed by means of an isothermal titration calorimeter VP Itc, Microcal at 25.0 °C. The calorimeter reaction cell was filled with adamantyl glycoside solution (V_0=1.42 cm^3; $c_0 \approx 5\times10^{-4}$ mol dm^{-3}) in water. The enthalpy changes were recorded upon stepwise additions (5 min intervals) of cyclodextrin aqueous solution ($c=5\times10^{-3}$ mol dm^{-3}). Blank

experiments were performed in order to make corrections for the enthalpy changes corresponding to the dilution of the titrant solution in pure water. All measurements were repeated at least three times.

4.8. Computational details

Since the size of the molecular systems modelled in this research (consisting up to 350 atoms) limited the use of the computationally demanding quantum-mechanical methods for conformational search, the combination of molecular mechanics and density functional theory was used. The scope of herein reported investigation was limited to one mannose derivative, β anomer, namely **10**β with (*S*)-absolute configuration of the chiral linker. The initial geometries were built in Chem3D (CambridgeSoft, Cambridge, MA) program and further modified in Maestro v9.1.[39] The relatively fast conformational search was performed with MacroModel v9.8 using several searching methods and force fields (e.g., OPLS_2005).[40,41] The density functional theory (DFT) calculations were performed with the Gaussian09.[42] The most stable conformers were optimized with B3LYP method and 6-31G(d) basis set,[43–45] already used in similar studies of cyclodextrins.[46,47] The ensembles of the most stable conformers were optimized at the same level of theory in water (using IEF-PCM for describing implicit solvent effects).[48,49] Results were visualized using GaussView[50] and Chem3D (CambridgeSoft, Cambridge, MA) programs. Vibrational frequencies were calculated for the most stable conformers to ensure they are true minima on the potential energy surface.

Acknowledgements

This research was supported by the Ministry of Science, Education and Sports of the Republic of Croatia (grants No. 119-1191344-3121, No. 119-1191342-2961 and No. 119-1191342-1339). Computational resources provided by Isabella cluster (isabella.srce.hr) at Zagreb University Computing Centre (SRCE) were used for this research.

References and notes

1. Dodziuk, H. *Cyclodextrins and Their Complexes. Chemistry, Analytical Methods, Applications*; Wiley-VCH: Weinheim, Germany, 2006.
2. Uekama, R.; Hirayama, F.; Irie, T. *Chem. Rev.* **1998**, *98*, 2045–2076.
3. Rekharsky, M. V.; Inoue, Y. *Chem. Rev.* **1998**, *98*, 1875–1917.
4. Connors, K. A. *Chem. Rev.* **1997**, *97*, 1325–1358.
5. Eftink, M. R.; Andy, M. L.; Bystrom, K.; Perlmutter, H. D.; Kristol, D. S. *J. Am. Chem. Soc.* **1989**, *111*, 6765–6772.
6. Rüdiger, V.; Eliseev, A.; Simova, S.; Schneider, H.-J.; Blandamer, M. J.; Cullis, P. M.; Meyer, A. J. *J. Chem. Soc., Perkin Trans. 2* **1996**, 2119–2123.
7. Carrazana, J.; Jover, A.; Meijide, F.; Soto, V. H.; Vázques Tato, J. *J. Phys. Chem. B* **2005**, *109*, 9719–9726.
8. Charbonnier, F.; Penades, S. *Eur. J. Org. Chem.* **2004**, 3650–3656.
9. Binkowski, C.; Lequart, V.; Hapiot, F.; Tilloy, S.; Cecchelli, R.; Monflier, E.; Martin, P. *Carbohydr. Res.* **2005**, *340*, 1461–1468.
10. Soto Telini, V. H.; Jover, A.; Carrazana Garcia, J.; Galantini, L.; Meijide, F.; Vasquez Tato, J. *J. Am. Chem. Soc.* **2006**, *128*, 5728–5734.
11. Godínez, L. A.; Schwartz, L.; Criss, C. M.; Kaifer, A. E. *J. Phys. Chem. B* **1997**, *101*, 3376–3380.
12. Harrison, J. C.; Eftink, M. R. *Biopolymers* **1982**, *21*, 1153–1166.
13. Zhang, B.; Breslow, R. *J. Am. Chem. Soc.* **1993**, *115*, 9353–9354.
14. Gelb, R. I.; Raso, I.; Alper, J. S. *Supramol. Chem.* **1995**, *115*, 279–285.
15. Antelo, A.; Alvarez Alchalde, M.; Jover, A.; Meijijde, F.; Galantini, L.; Tato, J. V. 13th International Conference of Synthetic Organic Chemistry.
16. Liu, J.; Obando, D.; Liao, V.; Lifa, T.; Cood, R. *Eur. J. Org. Chem.* **2011**, *46*, 1949–1963.
17. De Sousa, F. B.; Leite Denadai, A. M.; Lula, I. S.; Lopes, J. F.; Dos Santos, H. F.; De Almeida, W. B.; Sinisterra, R. D. *Int. J. Pharm.* **2008**, *353*, 160–169.
18. Sakina, H.; Abdelaziz, B.; Leila, N.; Imene, D.; Fatiha, M.; Eddine, K. D. *J. Incl. Phenom. Macrocycl. Chem.* **2012**, *74*, 191–200.
19. Tablet, C.; Minea, L.; Dumitrache, L.; Hillebrand, M. *Spectrochim. Acta, Part A* **2012**, *92*, 56–63.
20. Seridi, L.; Boufelfel, A. *J. Mol. Liq.* **2011**, *158*, 151–158.
21. Madi, F.; Khatmi, D.; Dhaoui, N.; Bouzitouna, A.; Abdaoui, M.; Boucekkine, A. *C. R. Chim.* **2009**, *12*, 1305–1312.
22. Passos, J. J.; Sousa, F. B.; Lula, I. S.; Barreto, E. A.; Lopes, J. F.; Almeida, W. B.; Sinisterra, R. D. *Int. J. Pharm.* **2011**, *421*, 24–33.
23. Taylor, M. E.; Drickamer, K. *Introduction to Glycobiology*, 2nd ed.; Oxford University Press: New York, NY, 2006.
24. Ribić, R.; Kovačević, M.; Petrović Peroković, V.; Gruić-Sovulj, I.; Rapić, V.; Tomić, S. *Croat. Chem. Acta* **2010**, *83*, 421–431.
25. Ribić, R.; Habjanec, L.; Vranešić, B.; Frkanec, R.; Tomić, S. *Chem. Biodivers.* **2012**, *9*, 777–788.
26. Lindhorst, T. K. *Essentials of Carbohydrate Chemistry and Biochemistry*, 2nd ed.; Wiley-VCH: Weinheim, Germany, 2003.
27. Taulier, N.; Chalikian, T. V. *J. Phys. Chem. B* **2006**, *110*, 12222–12224.
28. Jana, M.; Bandyopadhyay, S. *J. Phys. Chem. B* **2011**, *115*, 6347–6357.
29. Morel, J.-P.; Morel-Desrosires, N. *J. Solution Chem.* **1981**, *10*, 451–458.
30. Morel-Desrosires, N.; Morel, J.-P. *J. Solution Chem.* **1979**, *8*, 579–592.
31. Blokzijl, W.; Engberts, J. B. F. N. *Angew. Chem., Int. Ed. Engl.* **1993**, *32*, 1545–1579.
32. Franks, F. *Faraday Symp. Chem. Soc.* **1982**, *17*, 7–10.
33. Vicha, R.; Rouchal, M.; Kozubkova, Z.; Kurritka, I.; Marek, R.; Branna, P.; Cmelik, R. *Supramol. Chem.* **2011**, *23*, 663–677.
34. Li, J.-Ye.; Sun, D.-F.; Hao, A.-Y.; Sun, H.-Y.; Shen, J. *Carbohydr. Res.* **2010**, *345*, 685–688.
35. Heine, T.; Dos Santos, H. F.; Patchkowskii, S.; Duarte, H. A. *J. Phys. Chem. A* **2007**, *111*, 5648–5654.
36. Bader, R. F. W. *Atoms in Molecules: A Quantum Theory*; Oxford University Press: Oxford, UK, 1990.
37. Koch, U.; Popelier, P. L. A. *J. Phys. Chem.* **1995**, *99*, 9747–9754.
38. Popelier, P. L. A. *J. Phys. Chem. A* **1999**, *102*, 1873–1878.
39. Maestro v9.1; Schrödinger: New York, NY, 2011.
40. MacroModel, version 9.8; Schrodinger: New York, NY, 2010.
41. Mohamadi, F.; Richards, N. G. J.; Guida, W. C.; Liskamp, R.; Lipton, M.; Caufield, C.; Chang, G.; Henrickson, T.; Still, W. C. *J. Comput. Chem.* **1990**, *11*, 440–467.
42. Frisch, M. J.; Trucks, G. W.; Schlegel, H. B.; Scuseria, G. E.; Robb, M. A.; Cheeseman, J. R.; Scalmani, G.; Barone, V.; Mennucci, B.; Petersson, G. A.; Nakatsuji, H.; Caricato, M.; Li, X.; Hratchian, H. P.; Izmaylov, A. F.; Bloino, J.; Zheng, G.; Sonnenberg, J. L.; Hada, M.; Ehara, M.; Toyota, K.; Fukuda, R.; Hasegawa, J.; Ishida, M.; Nakajima, T.; Honda, Y.; Kitao, O.; Nakai, H.; Vreven, T.; Montgomery, J. A., Jr.; Peralta, J. E.; Ogliaro, F.; Bearpark, M.; Heyd, J. J.; Brothers, E.; Kudin, K. N.; Staroverov, V. N.; Kobayashi, R.; Normand, J.; Raghavachari, K.; Rendell, A.; Burant, J. C.; Iyengar, S. S.; Tomasi, J.; Cossi, M.; Rega, N.; Millam, J. M.; Klene, M.; Knox, J. E.; Cross, J. B.; Bakken, V.; Adamo, C.; Jaramillo, J.; Gomperts, R.; Stratmann, R. E.; Yazyev, O.; Austin, A. J.; Cammi, R.; Pomelli, C.; Ochterski, J. W.; Martin, R. L.; Morokuma, K.; Zakrzewski, V. G.; Voth, G. A.; Salvador, P.; Dannenberg, J. J.; Dapprich, S.; Daniels, A. D.; Farkas, Ö.; Foresman, J. B.; Ortiz, J. V.; Cioslowski, J.; Fox, D. J. *Gaussian 09, Revision A.1*; Gaussian: Wallingford, CT, 2009.
43. Becke, A. D. *J. Chem. Phys.* **1993**, *98*, 5648–5652.
44. Lee, C.; Yang, W.; Parr, R. G. *Phys. Rev. B* **1988**, *37*, 785–789.
45. Stephens, P. J.; Devlin, F. J.; Chabalowski, C. F.; Frisch, M. J. *J. Phys. Chem.* **1994**, *98*, 11623–11627.
46. Anconi, C. P. A.; Delgado, L. S.; Alves dos Reis, J. B.; Almeida, W. B.; Costa, L. A. S.; Santos, H. F. *Chem. Phys. Lett.* **2011**, *515*, 127–131.
47. Li, W.; Lu, B.; Chen, F.; Yang, F.; Wang, Z. *J. Mol. Struct.* **2011**, *990*, 244–252.
48. Cances, E.; Mennucci, B.; Tomasi, J. *J. Chem. Phys.* **1997**, *107*, 3032–3041.
49. Cances, E.; Mennucci, B. *J. Math. Chem.* **1998**, *23*, 309–326.
50. Dennington, R.; Keith, T.; Millam, J. *GaussView, version 5*; Semichem: Shawnee Mission, KS, 2009.